

The ORF4b-encoded accessory proteins of Middle East respiratory syndrome coronavirus and two related bat coronaviruses localize to the nucleus and inhibit innate immune signalling

Krystal L. Matthews,^{1*} Christopher M. Coleman,^{1*} Yvonne van der Meer,² Eric J. Snijder² and Matthew B. Frieman¹

¹Department of Microbiology and Immunology, University of Maryland at Baltimore, 685 West Baltimore St, Room 380, Baltimore, MD 21201, USA

²Molecular Virology Laboratory, Department of Medical Microbiology, Leiden University Medical Center, PO Box 9600, 2300RC Leiden, The Netherlands

Correspondence

Matthew Frieman
mfrieman@som.umaryland.edu

The recently emerged Middle East respiratory syndrome coronavirus (MERS-CoV), a betacoronavirus, is associated with severe pneumonia and renal failure. The environmental origin of MERS-CoV is as yet unknown; however, its genome sequence is closely related to those of two bat coronaviruses, named BtCoV-HKU4 and BtCoV-HKU5, which were derived from Chinese bat samples. A hallmark of highly pathogenic respiratory viruses is their ability to evade the innate immune response of the host. CoV accessory proteins, for example those from severe acute respiratory syndrome CoV (SARS-CoV), have been shown to block innate antiviral signalling pathways. MERS-CoV, similar to SARS-CoV, has been shown to inhibit type I IFN induction in a variety of cell types *in vitro*. We therefore hypothesized that MERS-CoV and the phylogenetically related BtCoV-HKU4 and BtCoV-HKU5 may encode proteins with similar capabilities. In this study, we have demonstrated that the ORF4b-encoded accessory protein (p4b) of MERS-CoV, BtCoV-HKU4 and BtCoV-HKU5 may indeed facilitate innate immune evasion by inhibiting the type I IFN and NF- κ B signalling pathways. We also analysed the subcellular localization of p4b from MERS-CoV, BtCoV-HKU4 and BtCoV-HKU5 and demonstrated that all are localized to the nucleus.

Received 25 November 2013

Accepted 16 January 2014

INTRODUCTION

A previously unknown coronavirus (CoV) has recently emerged in the Middle East causing 177 confirmed infections and 74 deaths, as of 4 January 2014 (van Boheemen *et al.*, 2012; Zaki *et al.*, 2012). This novel coronavirus, named Middle East respiratory syndrome CoV (MERS-CoV), is a lineage C betacoronavirus that is phylogenetically related to two bat coronaviruses, BtCoV-HKU4 and BtCoV-HKU5 (van Boheemen *et al.*, 2012; Woo *et al.*, 2006, 2007; Zaki *et al.*, 2012). The reservoir for MERS-CoV has not been identified; however, MERS-CoV genomic RNA has been detected in bat and dromedary camels in Qatar (Haagmans *et al.*, 2013; Memish *et al.*, 2013). BtCoV-HKU4 and BtCoV-HKU5 genome sequences were derived from RNA isolated from bat tissue; however, no live virus has ever been isolated for these viruses and they have not been grown in cell culture. All three viruses are also distantly related to severe acute respiratory syndrome CoV (SARS-CoV), the lineage B betacoronavirus that emerged from a bat reservoir in China in 2002/2003, causing severe respiratory illness and death in ~10% of the

~8000 infected individuals (van Boheemen *et al.*, 2012; Zaki *et al.*, 2012). Patients infected with MERS-CoV present with severe respiratory illness, as seen in SARS; however, additional symptoms, like renal failure, have also been reported (van Boheemen *et al.*, 2012; Zaki *et al.*, 2012).

The innate immune response is a first line of defence against viral infections and produces a broad antiviral response to inhibit virus replication and spread. One well-documented hallmark of SARS-CoV and other CoVs is their ability to evade innate immune responses (Frieman *et al.*, 2008). For example, we and others have identified several SARS-CoV proteins that block aspects of the innate immune response during SARS-CoV infection (Frieman *et al.*, 2007, 2009; Kamitani *et al.*, 2006; Kopecky-Bromberg *et al.*, 2007; Wathelet *et al.*, 2007; Zhao *et al.*, 2011). In infected cells, these proteins block the innate virus-sensing and signalling pathways; specifically the type I IFN signalling pathway, JAK1/STAT1, NF- κ B signalling and IFN-stimulated gene activation (Barretto *et al.*, 2005; Kamitani *et al.*, 2006; Niemeyer *et al.*, 2013; Sun *et al.*, 2012; Wang *et al.*, 2011; Züst *et al.*, 2011). The CoV accessory proteins (also known as group- or virus-specific proteins) are

*These authors have contributed equally.

strikingly different among CoV lineages and, in the case of SARS-CoV, encode many of the documented IFN antagonist activities (Frieman *et al.*, 2008). The genomes of MERS-CoV (Corman *et al.*, 2012), BtCoV-HKU4 (Woo *et al.*, 2006) and BtCoV-HKU5 (Woo *et al.*, 2006) are predicted to express a set of four such accessory proteins, encoded by ORF3, -4a, -4b and -5. Whilst they are at similar locations in the genome, comparison of the encoded protein sequences showed that they share only 30–47% amino acid identity and 47–62% amino acid similarity (Table 1). In this study, we found that the ORF4b-encoded accessory protein (p4b) of MERS-CoV (strain EMC/2012), BtCoV-HKU4 and BtCoV-HKU5 was able to inhibit IFN- β induction but only modestly inhibit the NF- κ B signalling pathway. We hypothesize that the ability to interfere with innate immune signalling is critically important to the pathogenesis of MERS-CoV. Additionally, the p4b protein of BtCoV-HKU4 and BtCoV-HKU5 can inhibit human innate immune pathways, which may contribute to their potential to become zoonotic human pathogens.

RESULTS

Expression of MERS-CoV, BtCoV-HKU4 and BtCoV-HKU5 p4b

The MERS-CoV ORF4b accessory gene was cloned downstream of the promoter of a pCAGGS-based vector such that ORF4b was fused in frame with sequences encoding either a C-terminal GFP tag or a C-terminal haemagglutinin (HA) tag. We also cloned the corresponding p4b-encoding accessory genes of BtCoV-HKU4 and BtCoV-HKU5 by amplification from the respective full-length cDNA copies of the viral genome. These plasmids were transfected into HEK293T cells and their expression levels were assessed by Western blot analysis using an anti-GFP (data not shown) or anti-HA (Fig. 1a) antibody. These data demonstrated robust expression of MERS-CoV, BtCoV-HKU4 and BtCoV-HKU5 p4b in our expression system.

Table 1. Percentage amino acid identity and similarity between MERS-CoV accessory proteins and BtCoV-HKU4 and BtCoV-HKU5

Each BtCoV-HKU4 and BtCoV-HKU5 accessory protein was compared with the homologous MERS-CoV accessory protein using CLUSTAL W for annotation of amino acid identity and similarity.

| Virus/gene | Aa identity/similarity (%) to: | |
|----------------|--------------------------------|------------|
| | BtCoV-HKU4 | BtCoV-HKU5 |
| MERS-CoV ORF3 | 42/51 | 42/57 |
| MERS-CoV ORF4a | 41/53 | 47/62 |
| MERS-CoV ORF4b | 30/47 | 31/49 |
| MERS-CoV ORF5 | 35/55 | 45/62 |

To establish p4b expression in MERS-CoV-infected cells, we produced a specific rabbit antiserum recognizing the C terminus of the native MERS-CoV p4b. This was an important control experiment, as genome sequence analysis (de Wilde *et al.*, 2013) and a study of the subgenomic transcripts produced by MERS-CoV (van Boheemen *et al.*, 2012) have suggested that ORF4b is not preceded by its own transcription regulatory sequence and would have to be expressed by 'leaky scanning' of ribosomes that would skip the ORF4a AUG codon while translating mRNA4. Using the p4b-specific antiserum, we were able to demonstrate robust expression of ORF4b in MERS-CoV-infected Vero and Huh7 cells by 9 h post-infection (p.i.) (Fig. 1b), when maximal viral RNA synthesis occurs (de Wilde *et al.*, 2013).

Subcellular localization of MERS-CoV, BtCoV-HKU4 and BtCoV-HKU5 p4b

We next sought to assess the subcellular localization of p4b of MERS-CoV, BtCoV-HKU4 and BtCoV-HKU5 by analysing its co-localization with Mitotracker (for mitochondria),

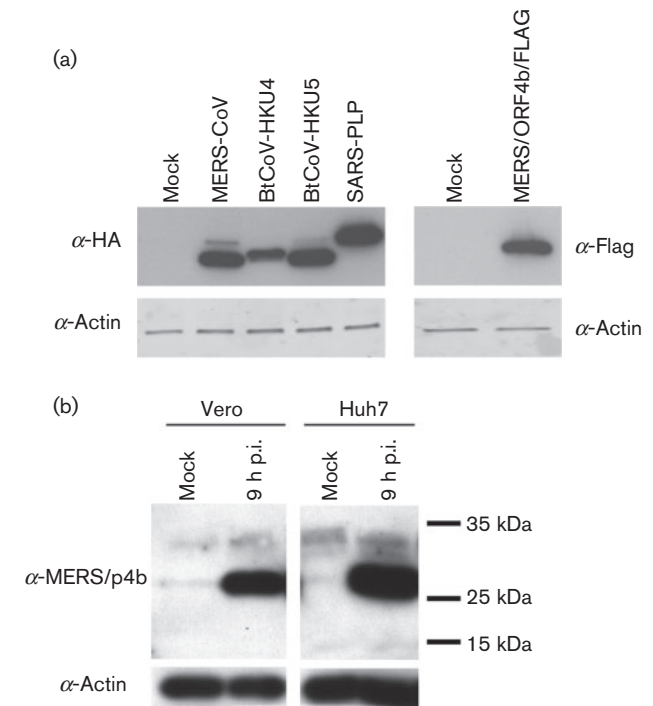


Fig. 1. Western blot analysis of the expression of MERS-CoV, BtCoV-HKU4 and BtCoV-HKU5 p4b. (a) HEK293T cells were transfected with the indicated plasmids and analysed by Western blotting with anti-HA, anti-Flag and anti-actin antibodies. Mock-transfected cells were used as negative control, and detection of cellular actin was used as a loading control. (b) Western blot analysis of ORF4b expression in MERS-CoV-infected Vero and Huh7 cells at 9 h post-infection (p.i.) using a p4b-specific rabbit antiserum. Mock-infected cells were used as negative control, and detection of cellular actin was used as a loading control.

Lysotracker (for lysosomes) or concanavalin A [for the endoplasmic reticulum (ER)] in transfected Vero E6 cells (Fig. 2). We found that MERS-CoV and BtCoV-HKU5 p4b localized strictly to the nucleus, and we did not observe co-localization with any of the specific organelle markers used (Fig. 2). BtCoV-HKU4 p4b localized to the nucleus with some minor cytoplasmic foci that did not co-localize with any of the specific organelles tested (Fig. 2).

Using the p4b-specific rabbit antiserum described above (Fig. 1b), we studied the expression and subcellular localization of p4b in MERS-CoV-infected Vero cells (Fig. 3). Cells were double labelled for p4b and dsRNA, a marker for viral RNA replication intermediates, and counterstained with Hoechst 33258 to label nuclear DNA. In these infected cells, the MERS-CoV p4b was readily detected from about 9 h p.i., with most of the signal localizing to the nucleus, in line with the results obtained during transient expression of the GFP-tagged version of the protein (Fig. 3). In cells fixed at 16 h p.i., the same nuclear staining pattern was observed as in cells fixed at an earlier stage of infection (data not shown). Additionally, we infected Huh7 cells and studied p4b localization at 9 and

16 h p.i. using the same anti-p4b antiserum. In these cells, p4b localized to the nucleus, identical to what is shown in Fig. 3 for Vero cells (data not shown).

Identification of nuclear localization signals (NLSs) in MERS-CoV, BtCoV-HKU4 and BtCoV-HKU5 p4b

Although the various p4b proteins analysed were only ~50 % similar and ~30 % identical in amino acid sequence, GFP-tagged versions of these proteins all localized to the nucleus (Fig. 2). This result was confirmed by analysing the localization of the native MERS-CoV ORF4b protein in infected cells (Fig. 3). We therefore sought to identify the NLSs of p4b. Bioinformatic analysis was conducted using cNLSMapper (http://nls-mapper.iab.keio.ac.jp/cgi-bin/NLS_Mapper_form.cgi) to identify putative NLSs. In all three orthologues, the presence of a bipartite NLS in the N-terminal domain of p4b was predicted by *in silico* analysis (Fig. 4a). We first deleted this entire domain of

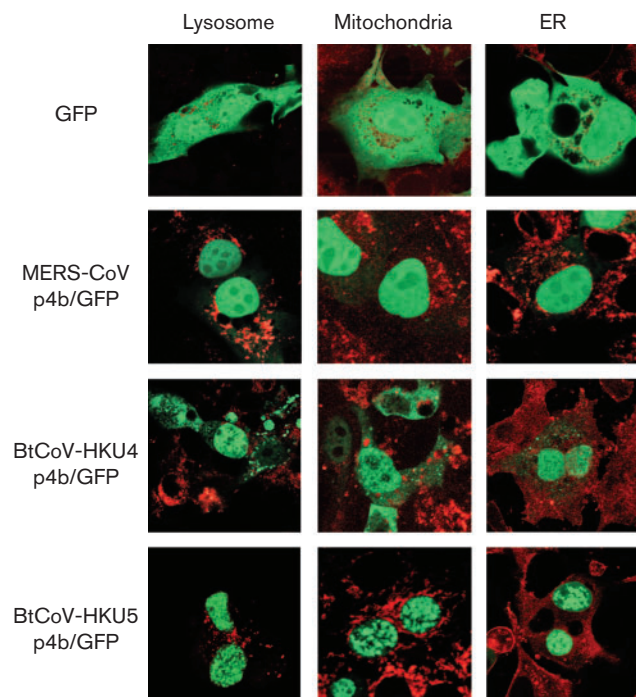


Fig. 2. Subcellular localization of MERS-CoV, BtCoV-HKU4 and BtCoV-HKU5 p4b in transfected cells. Plasmids expressing either GFP alone (green; top panel) or a GFP-tagged version of p4b of MERS-CoV, BtCoV-HKU4 and BtCoV-HKU5 were transfected into Vero E6 cells, which were double labelled using Lysotracker (a lysosomal marker), Mitotracker (a mitochondrial marker) or concanavalin A (an ER marker) (all staining red). Confocal microscopy images were produced for each stained slide with the red and green images merged onto one overlapping image. Bar, 25 μ m.

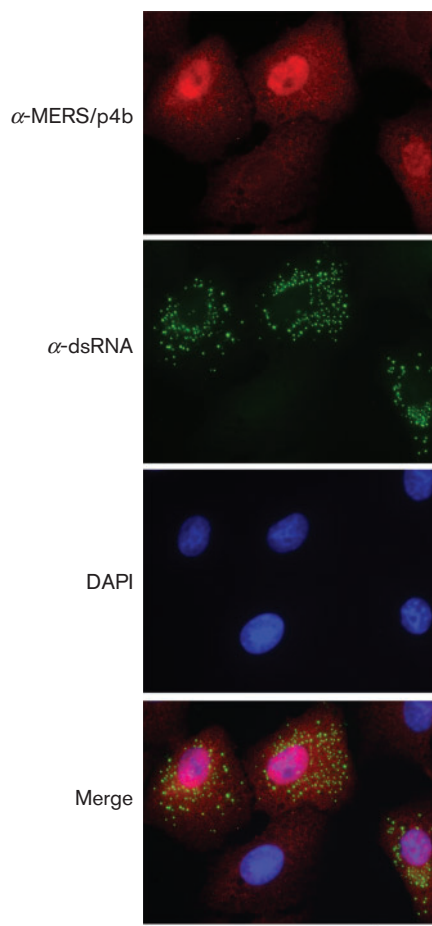


Fig. 3. Subcellular localization of MERS-CoV p4b in infected cells. Vero cells were infected with MERS-CoV, paraformaldehyde fixed at 9 h p.i. and double labelled for p4b and dsRNA, with nuclear DNA being stained with Hoechst 33258. Bar, 25 μ m.

each protein, including the predicted NLSs, to establish whether these regions indeed contained NLSs. These N-terminal truncated GFP-tagged p4bs were all retained in the cytoplasm (Fig. 4b), strongly suggesting that this region of the MERS-CoV, BtCoV-HKU4 and BtCoV-HKU5 p4b contains an NLS.

Bipartite NLSs are made up of two amino acid triplets of arginine and lysine separated by approximately 10 aa as shown in Fig. 4(a). The MERS-CoV, BtCoV-HKU4 and BtCoV-HKU5 p4bs all contained such a putative bipartite NLS. To further characterize these signals, we next mutated both 3 aa motifs of each NLS to a triple alanine, and each mutant ORF4b–GFP expression plasmid was transfected into Vero E6 cells.

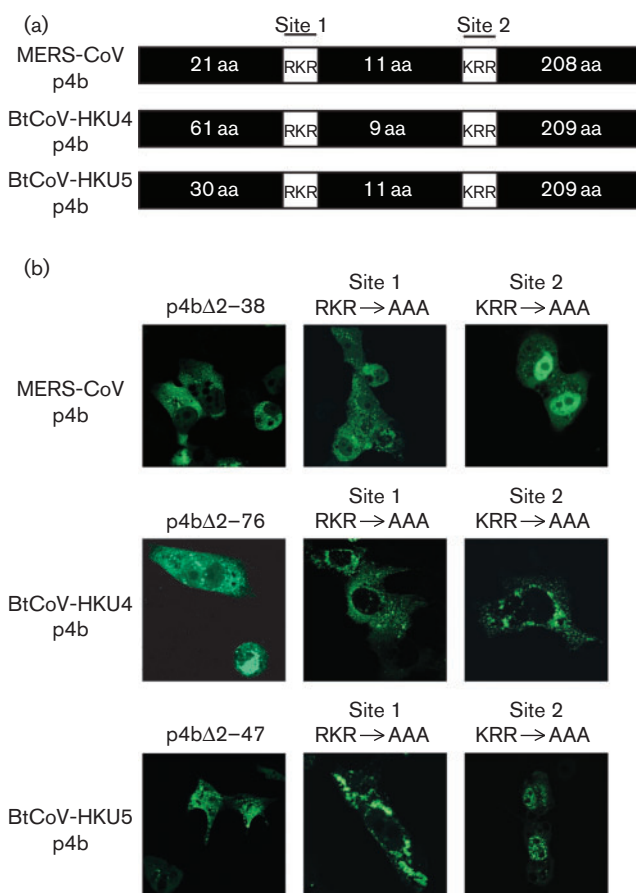


Fig. 4. NLS mapping in p4b. (a) Schematic of predicted NLSs in MERS-CoV, BtCoV-HKU4 and BtCoV-HKU5 p4b. Each protein has a predicted bipartite NLS (called site 1 and site 2). Both sites were targeted by replacing each of the basic amino acids with alanine and the effect on protein localization was analysed. (b) Plasmids expressing mutant p4b, either with deleted N-terminal domains or with alanine mutations at each NLS site, were transfected into Vero E6 cells, which were fixed and analysed by confocal microscopy. Shown are representative fluorescence microscopy images of transfected cells using the same labelling method as in Fig. 2.

When the site 1 RKR of the MERS-CoV p4b was changed to AAA, this abolished nuclear import; however, mutating the second site, KRR, to AAA did not completely abolish nuclear import (Fig. 4b). This suggested that the only NLS site in MERS-CoV p4b is predicted site 1 and not site 2. Similar results were obtained with the corresponding NLS mutants of BtCoV-HKU5 p4b (Fig. 4b). For the BtCoV-HKU4 p4b, we found that mutagenesis of either the predicted site 1 or site 2 abolished its nuclear localization (Fig. 4b), suggesting that this protein does indeed have a bipartite NLS. These data demonstrated that the N-terminal region of MERS-CoV, BtCoV-HKU4 and BtCoV-HKU5 p4b contains NLSs that may be important for their function in pathogenesis.

Inhibition of IFN- β promoter induction by MERS-CoV, BtCoV-HKU4 and BtCoV-HKU5 p4b

Cells respond to viral infection by inducing an innate immune response that is initiated by the induction of type I IFN expression. We examined the ability of MERS-CoV, BtCoV-HKU4 and BtCoV-HKU5 p4b to inhibit the induction of the innate immune signalling pathways leading to IFN- β gene induction and NF- κ B signalling. MERS-CoV does not induce a robust type I IFN response in infected cells (Zielecki *et al.*, 2013), similar to SARS-CoV (Kindler *et al.*, 2013). It is not known whether BtCoV-HKU4 or BtCoV-HKU5 inhibits innate immune signalling because these viruses have only been identified by bat sample sequencing and have never been isolated and studied as live viruses. However, in view of the percentage of sequence identity between the MERS-CoV, BtCoV-HKU4 and BtCoV-HKU5 accessory proteins, we hypothesized that these related viruses encode similar innate immune antagonists.

Using our GFP-tagged expression plasmids, we first assayed each p4b for its ability to inhibit IFN- β induction using a reporter assay with IFN- β promoter-driven expression of firefly luciferase. In the assay, HEK293T cells were transfected with the IFN- β /luciferase plasmid alone, or in combination with a plasmid encoding an N-terminally truncated RIG-I (N-RIG; a potent inducer of the IFN- β promoter) and either an empty GFP expression plasmid or a plasmid expressing the GFP-tagged p4b protein of MERS-CoV, BtCoV-HKU4 or BtCoV-HKU5. In addition, a positive-control plasmid encoding the SARS-CoV papain-like protease (PLP) was used, that we have reported previously inhibits IFN- β gene induction (Barretto *et al.*, 2006; Devaraj *et al.*, 2007; Frieman *et al.*, 2009; Sun *et al.*, 2012). At 18 h post-transfection, cells were analysed for the level of firefly luciferase expressed from the IFN- β /luciferase plasmid (Fig. 5a). We found that MERS-CoV p4b was a moderately strong inhibitor (fourfold) of RIG-I-dependent IFN- β promoter induction, whereas BtCoV-HKU4 and BtCoV-HKU5 p4b displayed moderate (2.5-fold) and strong (~50-fold) inhibition of RIG-I-dependent IFN- β promoter induction, respectively (Fig. 5a).

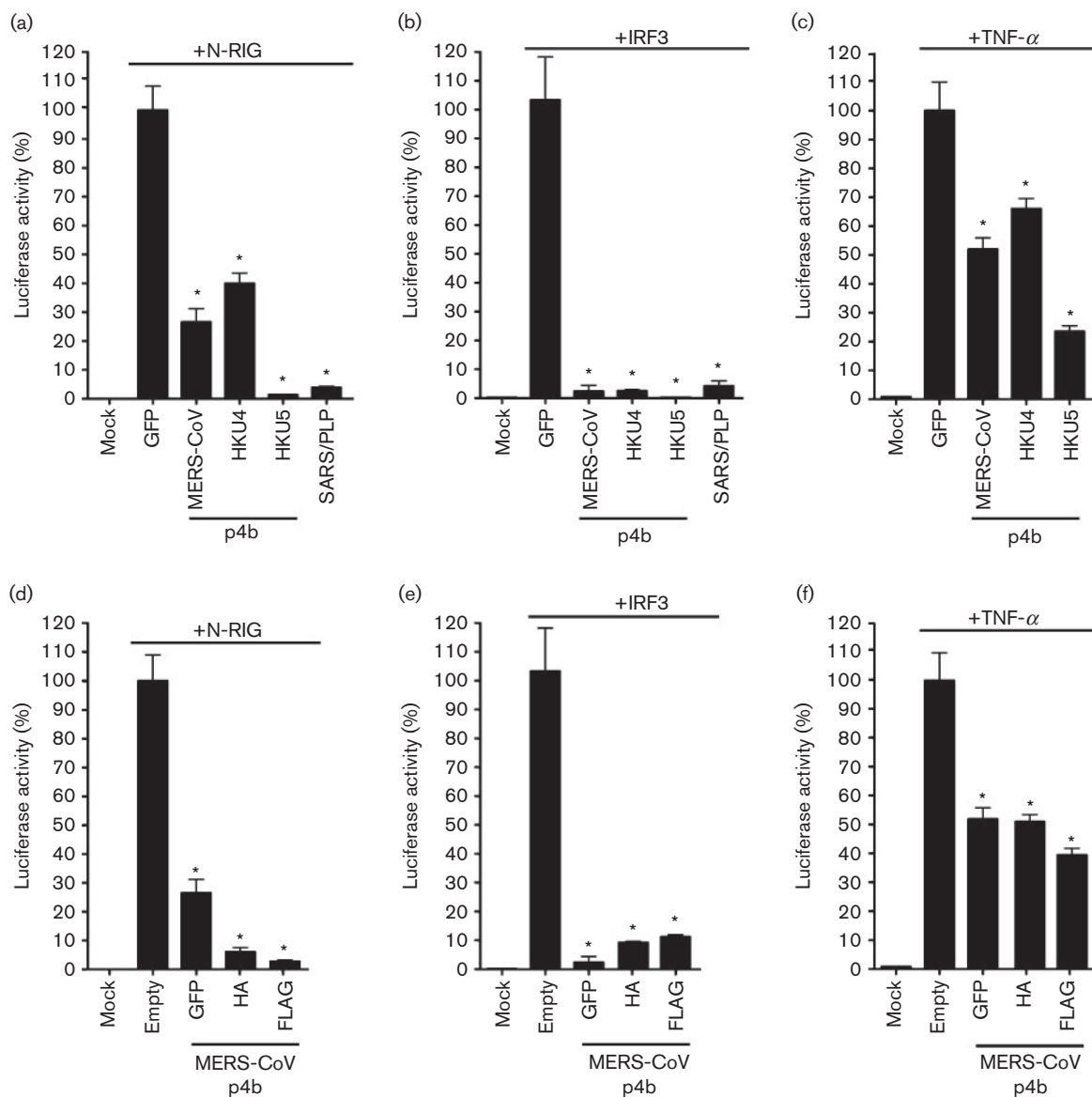


Fig. 5. Inhibition of IFN- β induction and NF- κ B signalling by p4b of MERS-CoV, BtCoV-HKU4 and BtCoV-HKU5. Plasmids expressing MERS-CoV, BtCoV-HKU4 or BtCoV-HKU5 ORF4b were tested for their ability to inhibit the induction of an IFN- β promoter/luciferase reporter induced by the N-terminally truncated RIG-I (N-RIG) (a, d) or IRF3 (b, e) or a NF- κ B-responsive luciferase reporter induced by TNF- α (c, f). The mean induction \pm SD across three transfections is shown relative to induction by the inducing plasmid alone (set at 100%). (a, d) 293T cells were transfected with plasmids encoding the IFN- β /luciferase reporter, N-RIG (a constitutive RIG-I mutant) and either empty vector or each of the accessory proteins of the three viruses in triplicate. (b, e) 293T cells were transfected with plasmids encoding the IFN- β /luciferase reporter, IRF3 and either empty vector or each of the accessory proteins of the three viruses in triplicate. (c, f) 293T cells were transfected with plasmids encoding the NF- κ B-responsive/luciferase reporter and either empty vector or each of the accessory proteins of the three viruses in triplicate. After 18 h, cells were treated with 10 ng TNF- α and incubated for an additional 6 h. Values that were significantly different from the control are indicated with an asterisk ($P < 0.05$).

We next analysed inhibition of IFN- β induction using IRF3 as the inducer rather than RIG-I (Fig. 5b). When IRF3 was overexpressed, there was a robust IFN- β -driven luciferase induction, which could be strongly inhibited by expression of

the GFP-tagged p4b from MERS-CoV, BtCoV-HKU4 or BtCoV-HKU5 (>50-fold inhibition by each). Taken together, these results demonstrated that p4b of MERS-CoV, BtCoV-HKU4 and BtCoV-HKU5 is a potent IFN antagonist.

Analysis of NF- κ B promoter inhibition by MERS-CoV, BtCoV-HKU4 and BtCoV-HKU5 p4b

The NF- κ B pathway is a critical signalling cascade that regulates innate immune responses. We hypothesized that MERS-CoV, BtCoV-HKU4 and BtCoV-HKU5 p4b would also inhibit NF- κ B signalling to block a potent antiviral response, as it does in the case of IFN- β signalling. Similar to the studies above, we utilized a NF- κ B reporter plasmid transfection system where the firefly luciferase gene is downstream of a promoter containing three NF- κ B-binding sites. This NF- κ B-responsive element is highly inducible by TNF- α in HEK293T cells (Fig. 5c). The NF- κ B/luciferase plasmid was transfected into HEK293T cells together with either an empty GFP expression plasmid or a plasmid expressing a GFP-tagged p4b of MERS-CoV, BtCoV-HKU4 or BtCoV-HKU5. At 18 h post-transfection, the cells were treated for 6 h with 10 ng TNF- α , which strongly induces the expression of NF- κ B-dependent genes. After 6 h of treatment, the cells were lysed and assayed for their level of firefly luciferase. As expected, TNF- α treatment induced NF- κ B signalling (Fig. 5c). Expression of MERS-CoV and BtCoV-HKU4 p4b resulted in only a twofold inhibition of NF- κ B signalling, whilst BtCoV-HKU5 p4b induced a fourfold inhibition. Although these results were statistically significant, they do not demonstrate robust inhibition of this pathway, compared with NF- κ B inhibition seen in previous studies (Frieman *et al.*, 2009). These data suggest that the MERS-CoV, BtCoV-HKU4 and BtCoV-HKU5 ORF4b protein is unlikely to be a potent inhibitor of the NF- κ B signalling pathway.

As GFP is a large globular protein and has a size comparable to that of p4b, we next sought to confirm that the C-terminal GFP tag was not having an effect on the activity of the p4b proteins. In the same luciferase assays as described above, C-terminally GFP-tagged MERS-CoV p4b was compared with C-terminally HA-tagged and N-terminally Flag-tagged MERS-CoV p4b (Niemeyer *et al.*, 2013). As shown in Fig. 4(d), there was a statistically significant difference in inhibition of N-RIG-induced IFN- β expression between GFP- and HA-tagged MERS-CoV p4b. However, we found that, for IRF3-induced IFN- β or TNF- α -induced NF- κ B, there was no significant difference with either tag (Fig. 5e, f). We also found that the moderate inhibition of NF- κ B signalling by GFP-tagged p4b was not due to the presence of a C-terminal tag, as the N-terminally Flag-tagged p4b had the same moderate activity. All together, these data demonstrated that the p4b proteins of MERS-CoV, BtCoV-HKU4 and BtCoV-HKU5 can inhibit specific innate immune signalling pathways in cells.

As the nuclear localization of p4b may be important in its function as an IFN antagonist, we sought to test p4b mutants from MERS-CoV, BtCoV-HKU4 and BtCoV-HKU5 in the IFN- β gene induction and NF- κ B signalling reporter assays described above. Interestingly, there was

no correlation between nuclear localization and p4b IFN antagonism (data not shown). MERS-CoV, BtCoV-HKU4 and BtCoV-HKU5 p4b mutants that no longer localized to the nucleus were still able to inhibit IFN- β gene induction and NF- κ B signalling. This suggested that the nuclear localization of p4b has other functions outside of innate immune inhibition and that the binding partners that p4b utilizes for this inhibition may reside in the cytoplasm.

DISCUSSION

As of 4 January 2014, there have been 177 confirmed cases of human infection with the recently emerged MERS-CoV, with 74 cases having a lethal outcome (<http://www.euro.who.int/en/home>). It is unknown whether MERS-CoV will produce a larger outbreak, similar to SARS-CoV, but in any case the MERS fatality rate among laboratory-confirmed cases is very high and of particular concern. Further dissection of the biology, replication strategy and pathogenesis of MERS-CoV and related CoVs is needed. Many viruses, including SARS-CoV, encode proteins that block innate immune signalling during infection to enhance virus replication (Frieman *et al.*, 2008). In SARS-CoV, we have previously identified eight proteins that appear to block one or more innate immune pathways (Frieman *et al.*, 2007, 2009; Kopecky-Bromberg *et al.*, 2007). The phylogenetically related BtCoV-HKU4 and BtCoV-HKU5 genome sequences were derived from bat samples in China; however, the viruses themselves have never been isolated. Therefore, direct comparison of viral infection among the three viruses is not possible. In lieu of live virus experiments, we focused on evaluating the innate immune antagonism activity of a related protein found in all three of the viruses, based on previous work showing that SARS-CoV accessory proteins can encode innate immune antagonists, which have also been shown to be important for pathogenesis *in vivo* (Frieman *et al.*, 2009; Zhao *et al.*, 2009).

A previous report by Niemeyer *et al.* (2013) also screened the MERS-CoV accessory proteins for their ability to inhibit innate immune induction. Whilst that report focused on the ORF4a-encoded protein as having strong IFN antagonist activities, the study did report that p4b displayed some innate immune inhibition. Differences between that study and ours may be due to the inducer of IFN used in their initial screen (total RNA from vesicular stomatitis virus-infected cells) versus the potent type I IFN inducer N-RIG that we used in this study, or to the effects of N-terminal versus C-terminal tags altering protein function. Additionally, the localization shown for transiently expressed p4b in their paper suggested both cytoplasmic and nuclear staining, whilst we saw definitive nuclear localization in such an expression system. More importantly, in live virus infection studies, we observed endogenous virally expressed p4b to have strict nuclear localization.

MERS-CoV, BtCoV-HKU4 and BtCoV-HKU5 p4b proteins are innate immune signalling inhibitors that localize to the nucleus

In this study, we showed that p4b of MERS-CoV, BtCoV-HKU4 and BtCoV-HKU5 is localized to the nucleus when tagged with GFP. As the addition of a large GFP tag may influence the protein's localization, we also analysed MERS-CoV p4b expression and targeting in infected cells and thus confirmed the nuclear localization of the native protein.

As all tested p4b proteins localized to the nucleus, we sought to map their NLSs *in vitro*. Bioinformatic analysis predicted a bipartite NLS in the p4b N-terminal domain, where NLS signals often are located. Deletion of this domain eliminated the nuclear localization of each p4b. We then mutagenized either site 1 or site 2 of the predicted NLS in each p4b and found that, for MERS-CoV and BtCoV-HKU5, only the first site was essential for nuclear localization, whereas for BtCoV-HKU4 p4b both sites were required. It is intriguing that MERS-CoV and BtCoV-HKU5 have evolved a single NLS signal sequence, whilst BtCoV-HKU4 required both sites for nuclear localization. This may be a hallmark of additional host protein-binding sites in these sequences or structural differences in the N termini of the different p4b proteins. It may also suggest that these proteins could function differently if expressed in bat versus human cells, shown here. Further dissection of the p4b NLS and nuclear import machinery is needed to understand the exact composition required for localization of p4b to the nucleus.

We went on to characterize the ability of MERS-CoV, BtCoV-HKU4 and BtCoV-HKU5 p4b proteins to inhibit IFN- β induction and NF- κ B signalling. To test IFN- β gene induction, we used a constitutively active RIG-I variant, called N-RIG, and IRF3 as inducers. We found that, in N-RIG and IRF3 induction experiments, expression of GFP-tagged MERS-CoV, BtCoV-HKU4 and BtCoV-HKU5 p4bs significantly inhibited RIG-I dependent IFN β induction, but were only able to moderately inhibit the NF- κ B signalling pathway. Additionally, we tested whether the nature and position of the fusion tag influenced MERS-CoV p4b function, but when comparing a C-terminal HA and N-terminal Flag tag to the GFP tag no significant differences were seen. Future experiments will aim to establish whether the localization of p4b affects the replication or pathogenesis of MERS-CoV.

Implications for pathogenesis

A common feature of viruses is their ability to evade immune responses, specifically the innate immune response (Haller *et al.*, 2007). To do so, viruses have evolved a variety of mechanisms, like expression of decoy proteins (for example, poxvirus CrmB; Alejo *et al.*, 2006; Brunetti *et al.*, 2003; Waibler *et al.*, 2009; Xu *et al.*, 2012) and inhibition of IFN induction (influenza virus NS1, Hatada *et al.*, 1999; SARS-CoV PLP, Barretto *et al.*, 2006; Frieman *et al.*, 2009),

all of which serve to limit the ability of the host to control virus replication. Importantly, some viral innate immune inhibitors are host specific: for example, ectromelia virus (mouse pox virus) expresses IFN antagonists that work in mouse cells but not in rabbit cells (Wang *et al.*, 2004), and by swapping the IFN antagonists from rabbit pox virus to mouse pox virus, the species tropism can be changed (Wang *et al.*, 2004). Although BtCoV-HKU4 and BtCoV-HKU5 have only been found in bats and not in humans, their accessory proteins are effective at inhibiting human antiviral signalling pathways *in vitro* (this study and Niemeyer *et al.*, 2013). MERS-CoV genomic RNA has been found in humans and bats (Memish *et al.*, 2013) and is phylogenetically closely related to the bat BtCoV-HKU4 and BtCoV-HKU5 (van Boheemen *et al.*, 2012; Woo *et al.*, 2006; Woo *et al.*, 2007; Zaki *et al.*, 2012), which suggests that a recent zoonotic shift from bats or camels to humans may have occurred. A related SARS-CoV-like virus isolated from Chinese horseshoe bats encodes an ORF6 protein homologous to that found in human SARS-CoV isolates (Lau *et al.*, 2005). We have previously shown that this bat SARS-CoV ORF6 product is able to inhibit STAT1 nuclear import, like the human SARS-CoV ORF6 protein (Frieman *et al.*, 2007).

The fact that CoVs of bat origin encode multiple proteins that are able to inhibit human innate immune signalling pathways may make an important contribution to their potential to cause disease upon zoonotic transfer. Increased surveillance of environmental reservoirs, particularly bat (Memish *et al.*, 2013) and rodent species (Corman *et al.*, 2014), will help identify additional CoVs and other potential human pathogens. Increased deep-sequencing capacity and respiratory virus screening in hospitals throughout the world will allow scientists to identify previously unidentifiable respiratory infections in patients. This type of continued surveillance and in-depth dissection of novel viral pathogens will reveal commonalities that may aid in identifying drug targets for future therapeutics.

METHODS

Cell lines, viruses, and plasmids. MERS-CoV strain EMC/2012 and Vero cells were kindly provided by the Erasmus Medical Center, Rotterdam, The Netherlands. All virus stocks were stored at -80°C until ready for use. All cells were purchased from the ATCC and were used for growing MERS-CoV EMC/2012, as well as for plaque assays to determine viral load. All cells were grown in minimal essential medium (Invitrogen) with 10% FBS (Atlanta Biologicals) and 1% penicillin/streptomycin (Gemini Bioproducts). HEK293T cells were purchased from ATCC, grown in Dulbecco's minimal essential medium (Invitrogen) with 10% FBS and 1% penicillin/streptomycin. Flag-tagged ORF4b was kindly provided by Marcel Müller (University of Bonn Medical Center, Bonn, Germany; Niemeyer *et al.*, 2013). Firefly luciferase plasmids containing the IFN- β or NF- κ B promoter and the GFP- and HA-tagged SARS-CoV PLP expression plasmids have been described previously (Frieman *et al.*, 2009).

Cloning of MERS-CoV, BtCoV-HKU4 and BtCoV-HKU5 ORF4b. MERS-CoV ORF4b was synthesized by Bio Basic without codon optimization, based on GenBank accession no. NC_019843.1. The

ORF was synthesized with 5' *EcoRI* and 3' *XmaI* sites for cloning into a pCAGGS/GFP or pCAGGS/HA vector (described by Frieman *et al.*, 2007). BtCoV-HKU4.2 and -HKU5 accessory ORF4b sequences were amplified from full-length cDNA clones generated and generously provided by Dr Ralph Baric (University of North Carolina at Chapel Hill, NC, USA). Primers were synthesized and fragments amplified for each ORF4b containing 5' *EcoRI* and 3' *XmaI* restriction sites for cloning into the same pCAGGS/GFP vector. Primers used for BtCoV-HKU4 cloning were 5'-gaattcaccATGGACGACTCGATGGATTGG-3' and 5'-cccgggGCGGCCAGGAAAGCAGGCACGATAG-3' (restriction sites indicated in lower case). Primers used for BtCoV-HKU5 cloning were 5'-gaattcaccATGGCTTTTTCGCCATCCCTGT-3' and 5'-cccgggAACTGTAAGCACGCTGGGTGCGATTA-3'.

Amino acid sequence comparisons between viruses. To derive the amino acid similarity and identity percentages reported in Table 1, the accessory ORFs were identified in MERS-CoV (GenBank accession no. NC_019843.1), BtCoV-HKU4 (GenBank accession no. NC_009019) and BtCoV-HKU5 (GenBank accession no. NC_009020). The product of each ORF was compared pairwise with the corresponding MERS-CoV ORF using CLUSTAL W.

Luciferase assays. Analysis of the induction of IFN- β - or NF- κ B-induced genes was performed using a luciferase reporter assay in HEK293T cells. Briefly, an expression construct containing firefly luciferase and either the IFN- β promoter (IFN- β /luciferase) or a promoter containing three copies of the NF- κ B-binding site (NF- κ B/luciferase) was co-transfected with either a GFP control plasmid or the designated plasmid. Transfections of reporter plasmids into HEK293T cells were performed with Lipofectamine LTX (Invitrogen) transfection reagent as directed by the manufacturer. For all transfections, 200 ng luciferase plasmid, 200 ng viral expression plasmid or empty vector and 200 ng inducer plasmid (total 600 ng per well) was used in each well of a 48-well plate with 1 μ l Lipofectamine LTX. At 18 h post-transfection, cells were lysed and assayed for luciferase expression using a Dual-Luciferase Reporter System (Invitrogen) following the manufacturer's instructions. The ratio of experimental treatment to control inducer (RIG-I, IRF3 or TNF- α) was plotted. All transfections were performed in triplicate and representative results of three experiments are presented.

Western blotting and antibodies. MERS-CoV, BtCoV-HKU4 and BtCoV-HKU5 accessory ORF4b expression plasmids were assayed for protein expression by Western blotting. HEK293T cells were transfected with 200 ng each plasmid using Lipofectamine LTX. At 18 h post-transfection, cells were lysed in NP-40 lysis buffer [50 mM Tris/HCl, pH 7.4, 150 mM NaCl, 1% NP-40, 2 mM EDTA and protease inhibitors (Complete Mini Protease Inhibitor; Roche)]. Lysates were then run on SDS-PAGE gels (NuPage; Invitrogen) and blotted onto PVDF membrane (Invitrogen). Proteins were visualized using anti-GFP antibody (Sigma-Aldrich), anti-HA (Sigma-Aldrich), anti-actin (Pierce), anti-Flag (Sigma-Aldrich) and HRP-conjugated secondary anti-rabbit antibody (GE Life Sciences). A MERS-CoV p4b-specific rabbit antiserum was ordered from Genscript and produced using as antigen a synthetic peptide representing the C-terminal 24 residues of the protein (SIRSSNQGNKQIVHSYPILHHPGF). The specificity of the antiserum was verified by Western blot analysis and immunofluorescence microscopy using samples from MERS-CoV-infected Vero or Huh7 cells, as described previously (de Wilde *et al.*, 2013), whilst using pre-immune serum and mock-infected cell lysates as negative controls.

Characterization of the subcellular localization of CoV accessory proteins by confocal microscopy. Vero E6 cells were seeded into 24-well plates (Corning) containing round coverslips (Fisher) and cultured overnight at 37 °C. Cells were transfected with 2 μ g DNA of each of the GFP-tagged accessory protein expression vectors

using the Lipofectamine LTX PLUS reagent protocol (Invitrogen) with optimization for Vero E6 cells. After overnight incubation at 37 °C, the cells were stained for mitochondria using Mitotracker Red CMXRos, for lysosomes using LysoTracker Red DND-99 or for the ER using concanavalin A conjugated to Alexa Fluor 594 (all dyes were from Invitrogen Molecular Probes). Cells were then fixed in 4% paraformaldehyde (Thermo Scientific) overnight at 4 °C and mounted onto slides using VectorShield mounting medium (Vector Laboratories).

Mitotracker was resuspended in anhydrous DMSO (Sigma-Aldrich) at a concentration of 1 mM and then diluted 1:2000 into normal Vero cell growth medium. The stain was then added to each well and the cells incubated for 2 h at 37 °C before being fixed. LysoTracker was diluted 1:15000 into normal Vero cell growth medium. The stain was added to each well and the cells incubated for 45 min at 37 °C before fixation.

To stain the ER, fixed cells were permeabilized using 0.1% Triton X-100 (Sigma-Aldrich) in PBS (Quality Biological) for 15 min at room temperature and blocked in 5% BSA (Sigma-Aldrich) in PBS for a further 5 min. Concanavalin A conjugated to Alexa Fluor 594 was resuspended in 0.1 M sodium bicarbonate (Gibco) at a concentration of 5 mg ml⁻¹ and then diluted 1:25 into PBS containing 1% BSA, 0.05% NP-40 (American Bioanalytical) and 2% normal goat serum (Vector Laboratories). The cells were incubated with the stain for 1 h at room temperature, with shaking. After washing three times in PBS containing 1% BSA and 0.05% NP-40, the coverslips were mounted onto slides using VectorShield mounting medium. The slides were viewed on an LSM510 confocal microscope (Zeiss) and analysed using ImageJ.

Using a specific rabbit antiserum, the subcellular localization of MERS-CoV p4b in infected Vero and Huh7 cells was analysed by immunofluorescence microscopy, as described previously (de Wilde *et al.*, 2013). All localization studies with live MERS-CoV were performed inside biosafety cabinets in a Biosafety Level 3 facility at Leiden University Medical Center.

ACKNOWLEDGEMENTS

We thank Dr Ralph Baric and Boyd Yount (University of North Carolina at Chapel Hill) for the BtCoV-HKU4 and BtCoV-HKU5 genome plasmids and Marcel Müller (University of Bonn, Germany) for the Flag-tagged MERS-CoV ORF4b. We are grateful to Adriaan de Wilde and Diederik Oudshoorn (LUMC) for assistance with experiments with live MERS-CoV and ORF4b expression analysis. We also thank the members of the Frieman and Snijder laboratories for their advice and assistance. This work was supported by NIH grant RO1 AI 095569-01 to M. B. F.

REFERENCES

- Alejo, A., Ruiz-Argüello, M. B., Ho, Y., Smith, V. P., Saraiva, M. & Alcami, A. (2006). A chemokine-binding domain in the tumor necrosis factor receptor from variola (smallpox) virus. *Proc Natl Acad Sci USA* 103, 5995–6000.
- Barretto, N., Jukneliene, D., Ratia, K., Chen, Z., Mesecar, A. D. & Baker, S. C. (2005). The papain-like protease of severe acute respiratory syndrome coronavirus has deubiquitinating activity. *J Virol* 79, 15189–15198.
- Barretto, N., Jukneliene, D., Ratia, K., Chen, Z., Mesecar, A. D. & Baker, S. C. (2006). Deubiquitinating activity of the SARS-CoV papain-like protease. *Adv Exp Med Biol* 582, 37–41.
- Brunetti, C. R., Paulose-Murphy, M., Singh, R., Qin, J., Barrett, J. W., Tardivel, A., Schneider, P., Essani, K. & McFadden, G. (2003). A

secreted high-affinity inhibitor of human TNF from Tanapox virus. *Proc Natl Acad Sci USA* 100, 4831–4836.

Corman, V. M., Eckerle, I., Bleicker, T., Zaki, A., Landt, O., Eschbach-Bludau, M., van Boheemen, S., Gopal, R., Ballhause, M. & other authors (2012). Detection of a novel human coronavirus by real-time reverse-transcription polymerase chain reaction. *Euro Surveill* 17, 20285.

Corman, V. M., Kallies, R., Philipps, H., Gopner, G., Muller, M. A., Eckerle, I., Brunink, S., Drosten, C. & Drexler, J. F. (2014). Characterization of a novel betacoronavirus related to MERS-CoV in European hedgehogs. *J Virol* 88, 717–724.

de Wilde, A. H., Raj, V. S., Oudshoorn, D., Bestebroer, T. M., van Nieuwkoop, S., Limpens, R. W., Posthuma, C. C., van der Meer, Y., Bárcena, M. & other authors (2013). MERS-coronavirus replication induces severe in vitro cytopathology and is strongly inhibited by cyclosporin A or interferon- α treatment. *J Gen Virol* 94, 1749–1760.

Devaraj, S. G., Wang, N., Chen, Z., Chen, Z., Tseng, M., Barretto, N., Lin, R., Peters, C. J., Tseng, C. T. & other authors (2007). Regulation of IRF-3-dependent innate immunity by the papain-like protease domain of the severe acute respiratory syndrome coronavirus. *J Biol Chem* 282, 32208–32221.

Frieman, M., Yount, B., Heise, M., Kopecky-Bromberg, S. A., Palese, P. & Baric, R. S. (2007). Severe acute respiratory syndrome coronavirus ORF6 antagonizes STAT1 function by sequestering nuclear import factors on the rough endoplasmic reticulum/Golgi membrane. *J Virol* 81, 9812–9824.

Frieman, M., Heise, M. & Baric, R. (2008). SARS coronavirus and innate immunity. *Virus Res* 133, 101–112.

Frieman, M., Ratia, K., Johnston, R. E., Mesecar, A. D. & Baric, R. S. (2009). Severe acute respiratory syndrome coronavirus papain-like protease ubiquitin-like domain and catalytic domain regulate antagonism of IRF3 and NF- κ B signaling. *J Virol* 83, 6689–6705.

Haagmans, B. L., Al Dhahiry, S. H., Reusken, C. B., Raj, V. S., Galiano, M., Myers, R., Godeke, G. J., Jonges, M., Farag, E. & other authors (2013). Middle East respiratory syndrome coronavirus in dromedary camels: an outbreak investigation. *Lancet Infect Dis* [Epub ahead of print].

Haller, O., Kochs, G. & Weber, F. (2007). Interferon, Mx, and viral countermeasures. *Cytokine Growth Factor Rev* 18, 425–433.

Hatada, E., Saito, S. & Fukuda, R. (1999). Mutant influenza viruses with a defective NS1 protein cannot block the activation of PKR in infected cells. *J Virol* 73, 2425–2433.

Kamitani, W., Narayanan, K., Huang, C., Lokugamage, K., Ikegami, T., Ito, N., Kubo, H. & Makino, S. (2006). Severe acute respiratory syndrome coronavirus nsp1 protein suppresses host gene expression by promoting host mRNA degradation. *Proc Natl Acad Sci USA* 103, 12885–12890.

Kindler, E., Jónsdóttir, H. R., Muth, D., Hamming, O. J., Hartmann, R., Rodriguez, R., Geffers, R., Fouchier, R. A., Drosten, C. & other authors (2013). Efficient replication of the novel human betacoronavirus EMC on primary human epithelium highlights its zoonotic potential. *MBio* 4, e00611–e00612.

Kopecky-Bromberg, S. A., Martínez-Sobrido, L., Frieman, M., Baric, R. A. & Palese, P. (2007). Severe acute respiratory syndrome coronavirus open reading frame (ORF) 3b, ORF 6, and nucleocapsid proteins function as interferon antagonists. *J Virol* 81, 548–557.

Lau, S. K., Woo, P. C., Li, K. S., Huang, Y., Tsoi, H. W., Wong, B. H., Wong, S. S., Leung, S. Y., Chan, K. H. & Yuen, K. Y. (2005). Severe acute respiratory syndrome coronavirus-like virus in Chinese horseshoe bats. *Proc Natl Acad Sci U S A* 102, 14040–14045.

Memish, Z. A., Mishra, N., Olival, K. J., Fagbo, S. F., Kapoor, V., Epstein, J. H., Alhakeem, R., Durosinioun, A., Al Asmari, M. & other authors (2013). Middle East respiratory syndrome coronavirus in bats, Saudi Arabia. *Emerg Infect Dis* 19, 1819–1823.

Niemeyer, D., Zillinger, T., Muth, D., Zielecki, F., Horvath, G., Suliman, T., Barchet, W., Weber, F., Drosten, C. & Müller, M. A. (2013). Middle East respiratory syndrome coronavirus accessory protein 4a is a type I interferon antagonist. *J Virol* 87, 12489–12495.

Sun, L., Xing, Y., Chen, X., Zheng, Y., Yang, Y., Nichols, D. B., Clementz, M. A., Banach, B. S., Li, K. & other authors (2012). Coronavirus papain-like proteases negatively regulate antiviral innate immune response through disruption of STING-mediated signaling. *PLoS ONE* 7, e30802.

van Boheemen, S., de Graaf, M., Lauber, C., Bestebroer, T. M., Raj, V. S., Zaki, A. M., Osterhaus, A. D., Haagmans, B. L., Gorbalenya, A. E. & other authors (2012). Genomic characterization of a newly discovered coronavirus associated with acute respiratory distress syndrome in humans. *MBio* 3, e00473-12.

Waibler, Z., Anzaghe, M., Frenz, T., Schwantes, A., Pöhlmann, C., Ludwig, H., Palomo-Otero, M., Alcamí, A., Sutter, G. & other authors (2009). Vaccinia virus-mediated inhibition of type I interferon responses is a multifactorial process involving the soluble type I interferon receptor B18 and intracellular components. *J Virol* 83, 1563–1571.

Wang, F., Ma, Y., Barrett, J. W., Gao, X., Loh, J., Barton, E., Virgin, H. W. & McFadden, G. (2004). Disruption of Erk-dependent type I interferon induction breaks the myxoma virus species barrier. *Nat Immunol* 5, 1266–1274.

Wang, G., Chen, G., Zheng, D., Cheng, G. & Tang, H. (2011). PLP2 of mouse hepatitis virus A59 (MHV-A59) targets TBK1 to negatively regulate cellular type I interferon signaling pathway. *PLoS ONE* 6, e17192.

Wathelet, M. G., Orr, M., Frieman, M. B. & Baric, R. S. (2007). Severe acute respiratory syndrome coronavirus evades antiviral signaling: role of nsp1 and rational design of an attenuated strain. *J Virol* 81, 11620–11633.

Woo, P. C., Lau, S. K., Li, K. S., Poon, R. W., Wong, B. H., Tsoi, H. W., Yip, B. C., Huang, Y., Chan, K. H. & Yuen, K. Y. (2006). Molecular diversity of coronaviruses in bats. *Virology* 351, 180–187.

Woo, P. C. Y., Wang, M., Lau, S. K. P., Xu, H., Poon, R. W. S., Guo, R., Wong, B. H. L., Gao, K., Tsoi, H. w. & other authors (2007). Comparative analysis of twelve genomes of three novel group 2c and group 2d coronaviruses reveals unique group and subgroup features. *J Virol* 81, 1574–1585.

Xu, R.-H., Rubio, D., Roscoe, F., Krouse, T. E., Truckenmiller, M. E., Norbury, C. C., Hudson, P. N., Damon, I. K., Alcamí, A. & other authors (2012). Antibody inhibition of a viral type I interferon decoy receptor cures a viral disease by restoring interferon signaling in the liver. *PLoS Pathog* 8, e1002475.

Zaki, A. M., van Boheemen, S., Bestebroer, T. M., Osterhaus, A. D. & Fouchier, R. A. (2012). Isolation of a novel coronavirus from a man with pneumonia in Saudi Arabia. *N Engl J Med* 367, 1814–1820.

Zhao, J., Falcón, A., Zhou, H., Netland, J., Enjuanes, L., Pérez Breña, P. & Perlman, S. (2009). Severe acute respiratory syndrome coronavirus protein 6 is required for optimal replication. *J Virol* 83, 2368–2373.

Zhao, L., Rose, K. M., Elliott, R., van Rooijen, N. & Weiss, S. R. (2011). Cell-type-specific type I interferon antagonism influences organ tropism of murine coronavirus. *J Virol* 85, 10058–10068.

Zielecki, F., Weber, M., Eickmann, M., Spiegelberg, L., Zaki, A. M., Matrosovich, M., Becker, S. & Weber, F. (2013). Human cell tropism and innate immune system interactions of human respiratory coronavirus EMC compared to SARS-coronavirus. *J Virol* 87, 5300–5304.

Züst, R., Cervantes-Barragan, L., Habjan, M., Maier, R., Neuman, B. W., Ziebuhr, J., Szretter, K. J., Baker, S. C., Barchet, W. & other authors (2011). Ribose 2'-O-methylation provides a molecular signature for the distinction of self and non-self mRNA dependent on the RNA sensor Mda5. *Nat Immunol* 12, 137–143.